Effect of Carbonate Formation on the Physical, Mechanical, and Fire Resistance Properties of $CaCO_3$-Mineralized Sengon Wood

Xhania Prameswara,[a] Lina Karlinasari ,[a,*] Subyakto ,[b] and Arinana [a]

Fast-growing sengon wood falls into the low durability and strength class. Enhancing the physical, mechanical, and fire-resistance properties of sengon can be an important step toward increasing its market value. This study aimed to determine the effectiveness of $CaCO_3$ formation in enhancing physical, mechanical, and fire-resistance properties of sengon wood. The wood was impregnated in two steps with calcium chloride ($CaCl_2$) and assisted potassium carbonate (K_2CO_3) at three concentrations (0.5, 1, and 2 mol/L). The results showed that the consequent $CaCO_3$ mineralization process at moderate concentrations improved wood properties. The concentrations of 0.5 and 1 mol/L showed optimal overall performance in improving the properties of sengon wood, with 0.5 mol/L offering potential advantages in terms of treatment efficiency. In particular, mechanical properties were increased by about 20% compared to the control. The use of $CaCO_3$ at 2 mol/L was less effective at improving mechanical properties. However, the physical and fire resistance properties were comparable to those of moderate concentrations of 0.5 mol/L and 1 mol/L. Based on this work, mineralization can be regarded as an alternative to improve wood properties, especially fire resistance, for environmentally friendly structural applications.

DOI: 10.15376/biores.21.2.5351-5369

Keywords: Environmentally friendly; Calcium carbonate; Mineralization; Moderate concentration; Wood properties

Contact information: a: Forest Products Science and Technology Study Program, Department of Forest Products, Faculty of Forestry and Environment, IPB University, Bogor, Indonesia; b: Research Center for Biomass and Bioproducts- National Research and Innovation Agency, Serpong, Indonesia;
** Corresponding author: karlinasari@apps.ipb.ac.id*

INTRODUCTION

Wood is a natural, organic, and renewable material that has been utilized in various applications for thousands of years (Dunningham and Sargent 2015). As a lignocellulosic material, wood presents significant opportunities for the development of sustainable, value-added industries. It contributes to carbon storage while helping to reduce global dependence on fossil fuels (Kraigher *et al*. 2023). In addition to its environmental benefits, wood has long been recognized and utilized by communities as a reliable construction material. In Indonesia, approximately 85% of the current wood supply is sourced from plantation forests (Haryanto *et al*. 2021).

Sengon (*Falcataria moluccana*) wood is a fast-growing species characterized by low durability and mechanical strength (Delucis 2016). These limitations are attributed to the generally lower quality of fast-growing wood, particularly in terms of density,

dimensional stability, and natural durability (Karlinasari *et al.* 2018). Therefore, material modifications are necessary to enhance its overall quality, durability, and commercial value. In addition, sengon wood generally exhibits relatively low density and a porous anatomical structure, which results in high permeability and thereby facilitates the penetration of treatment solutions into the wood matrix during impregnation processes (Rahayu *et al*. 2019; Rahayu *et al*. 2024).

With the advancement of technology, many methods have been developed to enhance wood properties. Wood modification is an effective method for improving dimensional stability, water resistance, and service life of wood (Hill 2006). Mineralization is an environmentally friendly method of wood modification that is still not widely used. This process can significantly reduce the flammability of wood (Merk *et al*. 2015). The primary challenge in wood mineralization is achieving deep and uniform mineral penetration into the wood structure as mineral particles tend to aggregate, which limits effective penetration (Matsunaga *et al*. 2019).

This study explored an environmentally friendly method called mineralization, which uses a calcium carbonate ($CaCO_3$) solution. Mineralization was selected because its thermal degradation does not produce toxic compounds (Tao *et al*. 2019) and it has the potential to enhance the strength, dimensional stability, and durability of wood without changing its natural properties (Merk *et al.* 2015). Historically, wood preservation using toxic chemicals has proven effective but poses risks to living organisms and the environment, highlighting the need for safer and more sustainable alternatives (Hill 2006; Shalbafan and Thoemen 2023). Mineralization is typically performed under vacuum conditions at various chemical concentrations, which facilitates deeper penetration of the mineral solution into the wood structure and ensures a more uniform deposition of inorganic particles within the cell walls (Huang *et al*. 2018; Pondelak *et al*. 2021; Repič *et al*. 2022). Calcium carbonate ($CaCO_3$) is the primary and most valuable mineral formed through biomineralization and naturally found in Earth's crust (Rodriguez-Navarro *et al*. 2012; Dhami *et al*. 2013; Kumari *et al*. 2016).

Mineralized wood is essentially a simplified alternative to fossilized or petrified wood. Petrified wood forms through a combination of permineralization fill the cellular cavities with minerals, where organic components are gradually replaced by inorganic minerals such as silica or calcium carbonate (Mustoe 2017; Mustoe *et al.* 2023). Potassium carbonate (K_2CO_3) was selected as the carbonate source in this study due to its high solubility, strong alkalinity, and efficient reactivity with calcium ions (Ca^{2+}) to promote the *in-situ* formation of calcium carbonate ($CaCO_3$) within wood microstructures. Compared to other carbonate salts, K_2CO_3 provides a stable and controllable pH environment that facilitates uniform mineral precipitation and deeper penetration into the wood matrix, particularly under vacuum-assisted conditions (Huang *et al*. 2018; Repič *et al.* 2022). Its ionic radius and high diffusivity allow potassium ions to move more easily through wood cell walls, enhancing carbonate ion availability for reaction with calcium salts such as $CaCl_2$. Moreover, K_2CO_3 does not introduce toxic residues, making it a more environmentally friendly reagent than sodium-based carbonates (Merk *et al*. 2015; Pondelak *et al*. 2021). Previous studies have also reported that the use of K_2CO_3 can yield finer $CaCO_3$ crystals with improved interfacial adhesion between the mineral phase and wood polymers, thereby enhancing both dimensional stability and mechanical performance of the treated wood (Tao *et al*. 2019; Matsunaga *et al*. 2019). This study aimed to evaluate the effect of K_2CO_3-assisted calcium carbonate ($CaCO_3$) mineralization on the physical and mechanical properties of sengon wood and to determine the optimum mineral

concentration for enhancing its strength and dimensional stability. Therefore, it is hypothesized that the high solubility and diffusivity of K_2CO_3 facilitate the penetration of carbonate ions into the anatomical cavities of sengon wood, promoting in-situ $CaCO_3$ precipitation within the wood microstructure.

EXPERIMENTAL

Materials

Logs of sengon wood (*Falcataria moluccana*) aged 6 years, with an average diameter of approximately 30 cm and a length of 200 cm, were cut into boards measuring 7 cm in thickness and 100 cm in length. The boards were air-dried at room temperature until reaching a moisture content of 20% to 25%, then oven-dried at 60 °C until a moisture content of 10% to 12%. The boards with stable moisture content were subsequently impregnated in stick form with dimensions of 2.5 × 2.5 × 100 cm**.**

The chemical reagents used were sodium hydroxide (NaOH, 99%), calcium chloride ($CaCl_2$, 94%), potassium carbonate (K_2CO_3, AGC 99%), and distilled water (aquadest) as the solvent.

Solution Preparation

Solutions of calcium chloride ($CaCl_2$) and potassium carbonate (K_2CO_3) were prepared by dissolving the respective chemicals in distilled water (aquadest) for three different concentrations: 0.5, 1, and 2 mol/L. The quantity of each chemical used for the respective concentrations is presented in Table 1.

Table 1. Chemical Requirements

Treatments	Concentration (mol/L)	Materials (g/L)
Calcium Chloride ($CaCl_2$)	0.5	55.4
	1	110.98
	2	221.96
Potassium Carbonate (K_2CO_3)	0.5	69.1
	1	138.2
	2	276.4

Impregnation Process

The wood samples, which had been cut into sticks (2.5 × 2.5 × 100) cm and conditioned to air-dry moisture content, were first soaked in a 1% sodium hydroxide (NaOH) solution for 10 h. NaOH pre-treatment removes extractives and slightly swells the wood cell wall, increasing porosity and ion-exchange sites to enhance Ca^{2+} penetration and promote uniform *in situ* $CaCO_3$ mineral formation (Xu *et al*. 2020; Merk *et al*. 2026). The control samples (untreated wood) were not subjected to NaOH pretreatment.

The first stage of impregnation was carried out using calcium chloride ($CaCl_2$) solution at three different concentrations (0.5, 1, and 2 mol/L) for 5 h under a pressure of 7 kgf/cm² (0.7 MPa). After this treatment, the samples were conditioned for 3 days at a temperature of approximately 20 °C and 65% relative humidity (RH).

Subsequently, the second impregnation stage was conducted using potassium carbonate (K_2CO_3) solution, with the same concentrations, durations, and pressure

conditions as in the first stage. Following this, the samples were conditioned for 24 h under the same environmental conditions (±20 °C, RH 65%), then oven-dried for 60 h at 60 °C until reaching a constant weight. No post treatment washing was applied after each stage of mineralization process.

The sequential impregnation of $CaCl_2$ and K_2CO_3 solutions resulted in the *in situ* formation of calcium carbonate ($CaCO_3$) precipitates within the wood structure. The impregnation procedure was adapted and modified from Zhang *et al*. (2022) and Repic *et al*. (2023). The chemical reaction is described in Eq. 1.

$$CaCl_2(aq) + K_2CO_3(aq) \rightarrow CaCO_3(s) + 2KCl(aq) \quad (1)$$

The mineralized stick samples were then cut into the size of the testing sample. Ten replications for each concentration treatment were taken to be analyzed for physical, mechanical properties and fire resistance.

Dimensional Stability

Density and weight percent gain

The effectiveness of the impregnation process can be evaluated by examining the Weight Percent Gain (WPG). The value of WPG is used to determine the percentage increase in weight of the wood sample after treatment compared to its initial oven-dry weight. This parameter reflects the amount of chemical retention in the wood, thereby indicating the level of chemical absorption and distribution resulting from the impregnation process. The density was calculated using Eq. 2,

$$\rho = \frac{m}{V} \quad (2)$$

where m is the oven-dry mass of the specimen (g) and V is the corresponding oven-dry volume (cm^3).

The WPG was calculated using Eq. 3,

$$WPG\ (\%) = \frac{W_1 - W_0}{W_0} \times 100 \quad (3)$$

where W_0 is the initial oven-dried weight of the sample before impregnation, and W_1 is the oven-dried weight of the sample after impregnation.

Water uptake

Water uptake (WU) is used to evaluate the hydrophobic performance and dimensional stability of wood after treatment. Lower WU values indicate that the impregnation process has successfully reduced the wood's affinity for moisture. Water uptake was calculated based on the weight difference before and after immersion in water for 24 h. The WU was calculated with Eq. 4,

$$WU\ (\%) = \frac{W_2 - W_1}{W_1} \times 100 \quad (4)$$

where W_2 is the sample weight after immersion in water for 24 h.

Anti-swelling efficiency

Anti-swelling efficiency (ASE) is a parameter used to evaluate the effectiveness of wood modification in reducing dimensional changes due to moisture. The ASE value

reflects how much the treatment has improved the wood's resistance to swelling compared to untreated wood. The ASE was calculated with Eq. 5:

$$ASE\ (\%) = \frac{S_u - S_t}{S_u} \times 100 \quad (5)$$

where S_u is the volume swelling of untreated wood sample, and S_t is the volume swelling of the treated wood.

Mechanical Testing

MOE and MOR

Mechanical testing was conducted using both non-destructive and destructive methods. The dynamic modulus of elasticity (MOEd) was determined non-destructively using a Fakopp® Microsecond Timer, which provides an estimate of wood stiffness. This was then verified through destructive testing to measure the static modulus of elasticity (MOEs) and modulus of rupture (MOR), using a Universal Testing Machine (UTM) Instron® type 3360. The loading test results were recorded automatically by the testing machine, and the data obtained were then processed using formulas in accordance with the Indonesian National Standard (SNI) 8853 (2019) adopting from ASTM D143 (2014). The MOEd (kg/cm^2) was calculated with Eq. 6,

$$MOEd = \frac{v^2 \times \rho}{g} \quad (6)$$

where v is the ultrasonic velocity (m/s) through the wood specimen, ρ is the density of the wood (kg/m^3), and g is the gravitational acceleration (9.81 m/s^2).

The MOEs was calculated with Eq. 7,

$$MOEs = \frac{\Delta P L^3}{4bh^3 \Delta Y} \quad (7)$$

where ΔP is the change in load under proportional limit (N), L is the span length (mm), b is the width (mm), h is the thickness (mm) of the specimen, and ΔY is the change in deflection (mm).

The MOR (kg/cm^2) was calculated with Eq. 8,

$$MOR = \frac{3PL}{2bh^2} \quad (8)$$

where P is the maximum load applied at failure (N), L is the span length between supports (mm), b is the width of the specimen (mm), and h is the thickness of the specimen (mm).

Compressive strength and hardness

The compressive strength parallel to the grain was tested by placing the specimen on a Universal Testing Machine, followed by loading at a constant rate of 5.000000 pts/s. The hardness test was conducted using the same machine, where a steel ball with a surface area of 1 cm^2 was pressed into the specimen at the same loading rate. The compressive strength was calculated with Eq. 9,

$$\sigma_c = \frac{P}{A} \quad (9)$$

where P is the maximum load at failure (kg) and A is the cross-sectional area of the specimen (cm^2).

The hardness was calculated with Eq. 10,

$$H = \frac{P}{A} \quad (10)$$

where P is the applied load (kg) and A is the area of indentation (cm²).

Fire Resistance Test

The fire resistance test was conducted in accordance with ASTM E69-22 (2022) in modified, with ten replications for each concentration treatment. Prior to testing, all specimens had a moisture content below 15% and were weighed to determine their initial mass (W_b). The specimens, with dimensions of (31 × 1.905 × 0.9525) cm were then placed in a fire tube apparatus as described by Fouladi *et al.* (2015), and each specimen was positioned vertically during the test.

A thermocouple probe was attached to the upper end of the specimen and near the burner flame to measure the temperature and heat release (Fig. 1a). The burner used was a low-pressure Bunsen type with an inner tube diameter of 9.5 mm, mounted on a ring stand. It was equipped with a gas flow control system to ensure a stable flame throughout the test. The detailed specifications of the burner hood are presented in Fig. 1b.

The combustion temperature was maintained at approximately 700 °C, and each specimen was exposed to the flame for 4 min, with the flame tip positioned 4 cm below the lower end of the specimen. After 4 min, the combustion process was stopped, and the maximum temperature as well as the burning duration of each specimen were recorded. Subsequently, the specimens were weighed to determine their final mass after burning (W_s). The weight loss (%) was then calculated according to Eq. 11:

$$WL\ (\%) = \frac{W_b - W_s}{W_b} \times 100 \quad (11)$$

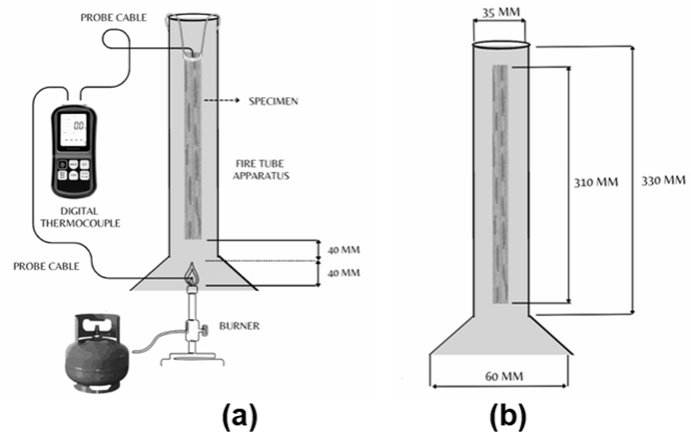

Fig. 1. Fire resistance experimental setup: (a): detailed specifications of the specimen and fire tube apparatus (b)

Pores Characterization

The mineralized sengon wood was analyzed using Scanning Electron Microscopy (SEM). SEM was used to observe the penetration and distribution of $CaCO_3$ crystals within the cell walls. Impregnated and control specimens were mounted on conductive adhesive, gold-coated, and examined under SEM with an accelerating voltage of 15 kV, chamber pressure between 10 and 400 Pa, low-vacuum mode, and a working distance of 8 mm. X-

ray diffraction (XRD) analysis was performed to evaluate the crystal structure characteristics of the samples using an Aeris PANalytical X-ray diffractometer. The diffraction angle was recorded over a 2θ range of 10° to 80° with a scanning speed of 0.2°/s.

Statistical Analysis

Descriptive statistics were calculated and presented as mean values with their corresponding standard deviations. Prior to statistical analysis, the normality of the data distribution was evaluated using the Shapiro–Wilk test, while the homogeneity of variances was assessed using Levene's test to ensure that the assumptions for parametric analysis were met. A one-way analysis of variance (ANOVA) was applied to evaluate the effect of mineralization concentration on the physical and mechanical properties of the treated wood. When significant differences were detected ($P < 0.05$), the means were further compared using Duncan's Multiple Range Test (DMRT) to identify statistically distinct treatment groups. Mean values followed by different superscript letters indicate significant differences ($P < 0.05$) according to DMRT. All statistical analyses were conducted using IBM SPSS Statistics (Version 29.0.0; IBM Corp., Armonk, NY, USA).

RESULTS AND DISCUSSION

Dimensional Stability

Density and weight percent gain

According to Fig. 2, the impregnation process increased wood density. This indicates that the solution successfully penetrated the wood structure and formed precipitates. Wood density increased by an average of approximately 18%, with the most pronounced improvement at 0.5 mol/L (21%). The 1 mol/L and 2 mol/L increases in concentration resulted in slightly lower density gains of 18% and 16%, respectively. This pattern indicates that mineralization concentrations of 0.5 ml/L were more effective at filling voids and increasing overall wood density. A similar phenomenon was also reported by Chen *et al*. (2020) and Holy *et al*. (2022). The study explained that the success of the mineralization process is greatly influenced by the homogeneity of the dispersion and the ability of minerals to penetrate the wood structure. Recent studies by Hernández *et al.* (2025) and Zhang *et al.* (2022) confirmed that $CaCO_3$ mineralization can increase the density and dimensional stability of wood. However, the effect is not always linear with increasing solution concentration, as excessive mineral content may lead to particle agglomeration that limits effective penetration. This interpretation is supported by SEM observations (Figs. 10g and 10h), which show that $CaCO_3$ crystals tend to aggregate on the wood surface, while minimal deposition occurs within the pores or lumens.

Figure 3 shows that the WPG of the $CaCO_3$ mineralized wood was 22.8%, 19.5%, and 16.2% for concentrations of 0.5, 1, and 2 mol/L, respectively. The slight decrease in WPG with increasing mineralization concentration indicates that excessively high concentrations may reduce the penetration of mineral ions into the wood structure due to pore blockage or premature surface precipitation. These results suggest that both 0.5 mol/L and 1 mol/L treatments provide relatively effective mineral deposition within the wood matrix compared to the 2 mol/L treatment. This trend aligns with the density pattern, in which mineral absorption efficiency was optimal at low concentrations. In contrast, at high concentrations, precipitation on the surface or pore saturation can inhibit the diffusion of ions into the interior of the wood tissue, as excessive mineral concentration leads to $CaCO_3$

agglomeration that clogs the wood surface and obstructs the grain ducts, preventing deeper mineral penetration (Liang *et al*. 2022). Similar results were reported by Li *et al*. (2022) and Hernandez *et al*. (2022, 2025).

Water uptake

Mineralized wood tends to be more hygroscopic and absorbs water more readily, while also improving dimensional stability and fire resistance because the mineral particles fill structural gaps and strengthen the wood tissue (Pondelak *et al*. 2021). In general, the mineralization process increases water absorption during submersion tests (Repic *et al*. 2022). The results in Fig. 3 show the water uptake (WU) of mineralized wood, which increased relative to controls at 71.42% (0.5 mol/L), 66.50% (1 mol/L), and 74.05% (2 mol/L). No significant difference among the concentrations was observed. Similar increases in WU after $CaCO_3$ mineralization have also been reported by Moya *et al*. (2020). In addition, the stability of deposited minerals during water exposure may influence water uptake, as leaching processes can alter the hygroscopic behavior of wood and increase its water absorption capacity (Dvořák *et al.* 2023; Jirouš-Rajković and Miklečić 2021). The ability of wood to absorb and release moisture causes its moisture content to fluctuate in response to environmental temperature and humidity (Iswanto 2018). Meanwhile, the anti-swelling efficiency (ASE) is used to evaluate the improvement in dimensional stability of treated wood.

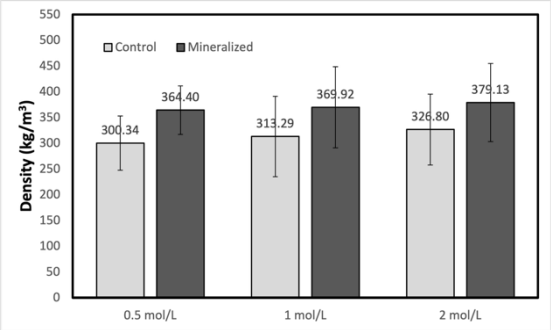

Fig. 2. Density enhancement of wood through $CaCO_3$ mineralization treatment

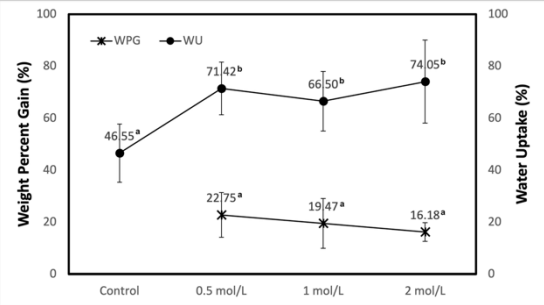

Fig. 3. Effect of mineralization concentration on the weight percent gain (WPG) and hygroscopic response of wood as water uptake (WU). Different superscript letters indicate significant differences ($P < 0.05$)

Anti swelling efficiency

The anti-swelling efficiency (ASE) values of the $CaCO_3$ mineralized wood samples were 38.5%, 37.6%, and 18.4% for concentrations of 0.5, 1, and 2 mol/L, respectively (Fig. 4).

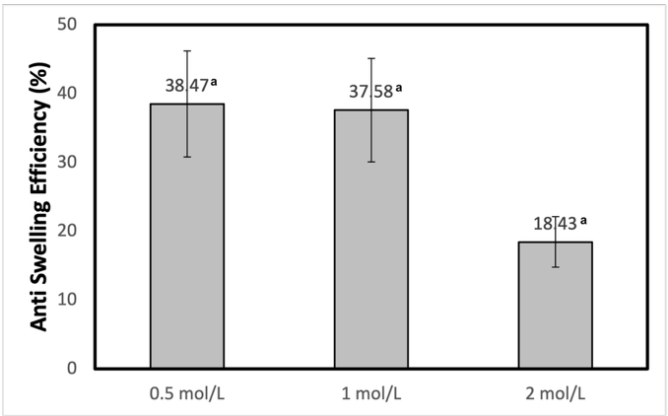

Fig. 4. Effect of $CaCO_3$ mineralization concentration on the anti-swelling efficiency (ASE) of sengon wood. Different superscript letters indicate significant differences ($P < 0.05$)

The relatively high ASE values at lower concentrations indicate that mineral impregnation effectively reduced the dimensional expansion of wood caused by water absorption. Although mineralized wood exhibited increased hygroscopicity and higher water uptake compared to the control, it still maintained good resistance to swelling. This suggests that $CaCO_3$ deposition within the wood structure helps to stabilize the cell walls, thereby limiting volumetric changes despite enhanced moisture interaction. However, mineralized wood tends to be more responsive to ambient humidity and temperature variations, adapting its moisture content to environmental conditions. These findings align with previous studies reporting that higher ASE values correspond to improved dimensional stability of wood (Hasnah 2019; Laksono *et al*. 2023).

Mechanical Tests

MOE and MOR

Previous studies have demonstrated a strong correlation between the dynamic modulus of elasticity (MOEd) and the static modulus of elasticity (MOEs) in wood. The MOEd values, which are obtained through non-destructive vibration or ultrasonic testing, are generally higher than those measured through static bending tests due to the absence of time-dependent deformation effects during dynamic loading (Divós and Tanaka 2005; Karlinasari *et al.* 2008; Hassan *et al*. 2013; Madhoushi and Boskabadi 2019). These findings indicate that dynamic testing methods can effectively predict the stiffness and mechanical performance of wood, as the results strongly correspond to those obtained from conventional static evaluations.

The results in Fig. 5 show that both the MOEd and MOEs of mineralized wood increased compared with the control, with the highest values observed at a $CaCO_3$ concentration of 0.5 mol/L (6310 MPa for MOEd and 6110 MPa for MOEs). The 0.5 mol/L treatment exhibited a significantly higher MOE than the control ($P < 0.05$).

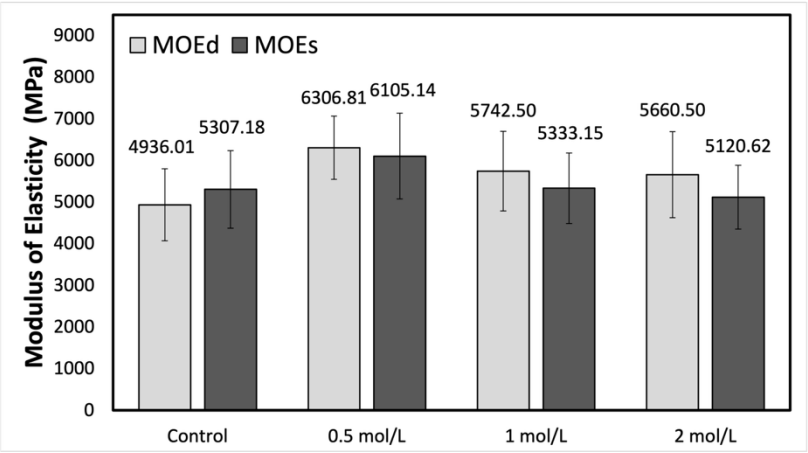

Fig. 5. Comparison of the modulus of elasticity dynamic (MOEd) and static (MOEs) between control and $CaCO_3$ mineralized wood

In contrast, the 1 and 2 mol/L treatments produced moderate increases that were not statistically different from the 0.5 mol/L sample according to Duncan's multiple range test (Table 2). The MOEd increased by 27.74%, 16.24%, and 14.67% for concentrations of 0.5, 1, and 2 mol/L, respectively, while the MOEs increased by 15.04% and 0.49% at 0.5 and 1 mol/L, but slightly decreased by 3.52% at 2 mol/L. These results confirm previous findings that the MOEd is typically higher than the MOEs. This difference occurs because the dynamic test measures the immediate elastic response of the wood during vibration, while the static test is affected by slower deformation that happens under constant loading.

The finding of this study indicates that wood mineralization at moderate concentrations can strengthen the cell wall structure by filling pores and forming bonds between minerals and cellulose and lignin components, thereby increasing material stiffness, in line with He et al. 2024. Meanwhile, Moya *et al*. (2020) stated that at higher concentrations, excess mineral ions can cause internal stress and an irregular mineral distribution, thereby reducing the effectiveness of reinforcement. The pattern of differences between MOEd and MOEs is also consistent with previous studies, which found that dynamic testing tends to yield higher modulus values than static testing due to wood's viscoelastic response (Arriaga *et al*. 2023). Overall, these results support that wood mineralization at optimal concentrations can improve mechanical properties without compromising structural integrity (Hernandez *et al*. 2025).

The modulus of rupture (MOR) values of the $CaCO_3$ mineralized wood samples were 14.7 MPa (control), 20.8 MPa (0.5 mol/L), 18.9 MPa (1 mol/L), and 17.2 MPa (2 mol/L) (Fig. 6). The mineralization treatment markedly increased the bending strength of wood compared to the control, with the highest improvement observed at 0.5 mol/L, showing a significant increase of approximately 41%. This enhancement can be attributed to the formation of mineral deposits that fill the lumens and cell walls of the wood, thereby strengthening fiber bonding and improving stress transfer efficiency (He *et al*. 2024). However, at higher concentrations (1 and 2 mol/L), the MOR values decreased slightly, which may be due to excessive mineral accumulation causing internal stress and non-uniform distribution within the wood structure (Moya *et al*. 2020; Soini *et al*. 2022). These findings are consistent with previous studies indicating that an optimal level of

mineralization enhances the MOE and MOR of wood without damaging its microstructure (Hernandez *et al*. 2025).

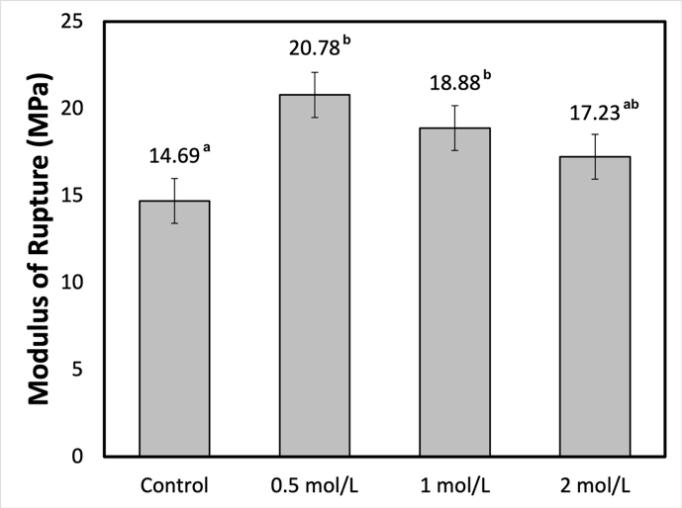

Fig. 6. Effect of $CaCO_3$ mineralization concentration on the modulus of rupture (MOR) of wood. Different superscript letters indicate significant differences ($P < 0.05$).

Compression strength and hardness

The compression strength of $CaCO_3$-mineralized wood increased markedly compared to the control, from 24.9 MPa (control) to 31.0 MPa at 0.5 mol/L and reaching the highest value of 32.7 MPa at 1 mol/L, before slightly decreasing to 29.1 MPa at 2 mol/L (Fig. 7). Similarly, the hardness values on Fig. 8 showed a comparable trend, increasing from 18.3 MPa (control) to 23.2 MPa at 0.5 mol/L, slightly decreasing at 1 mol/L (22.9 MPa), and further declining at 2 mol/L (22.4 MPa). This pattern suggests that mineralization at moderate concentrations (0.5 to 1 mol/L) provided optimal reinforcement to the wood structure, enhancing both compressive strength and surface hardness. The improvement can be attributed to the penetration and deposition of inorganic minerals within the cell walls and lumina, which increase density and fiber compactness (Garskaite *et al*. 2023; Choi *et al*. 2024; He *et al*. 2024). These findings are consistent with previous studies reporting that mineral reinforcement in wood improves its mechanical performance through the formation of interfacial bonds between mineral particles and the cellulose matrix (Soini *et al*. 2025). However, at higher concentrations (2 mol/L), excessive mineral accumulation may induce internal stress or microcracks, leading to a reduction in mechanical strength (Moya *et al*. 2020; Jiang *et al*. 2022). This trend aligns with the delignification–mineralization–densification mechanism described by Li *et al*. (2023), which demonstrated that controlled mineral deposition effectively enhances both compressive strength and hardness of modified wood.

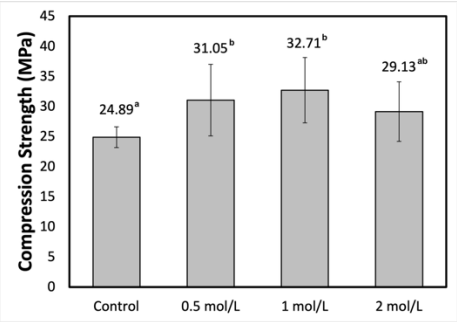

Fig. 7. Compression strength of wood after $CaCO_3$ mineralization treatment. Different superscript letters indicate significant differences ($P < 0.05$).

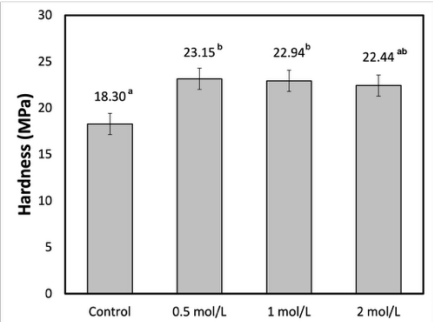

Fig. 8. Surface hardness of wood after $CaCO_3$ mineralization treatment. Different superscript letters indicate significant differences ($P < 0.05$).

Referring to Table 2, the mechanical properties of $CaCO_3$-mineralized wood showed significant improvement at a concentration of 0.5 mol/L across all tested parameters.

Table 2. Statistical Analysis (Duncan Test) of Physical and Mechanical Properties

Wood Properties	Values			
	Control	0.5 mol/L	1 mol/L	2 mol/L
WPG (%)	-	22.75^{a}	19.47^{a}	16.18^{a}
WU (%)	46.55^{a}	71.42^{b}	66.50^{b}	74.05^{b}
ASE (%)	-	38.47^{a}	37.48^{a}	18.43^{a}
MOEd (MPa)	4936.01^{a}	6306.81^{b}	5742.50^{ab}	5660.50^{ab}
MOEs (MPa)	5307.18^{ab}	6105.14^{b}	5333.15^{ab}	5120.62^{a}
MOR (MPa)	14.69^{a}	20.78^{b}	18.88^{b}	17.23^{ab}
Compression Strength (MPa)	24.89^{a}	31.05^{b}	32.71^{b}	29.31^{ab}
Hardness (MPa)	18.30^{a}	23.15^{b}	22.94^{b}	22.44^{a}

Notes: Means with different letters in the same column are significantly different at $P < 0.05$ according to Duncan's multiple range test.

In general, the optimal mineralization concentrations that enhanced the mechanical properties were observed at 0.5 and 1 mol/L compared to the control. This indicates that moderate mineral concentrations promoted effective mineral penetration and deposition within the wood structure, leading to improved density and mechanical reinforcement. This trend is consistent with the increase in density observed in Fig. 1, where mineralized wood at 0.5 and 1 mol/L exhibited greater density enhancement than samples treated at 2 mol/L. These results suggest that excessive mineral concentration may hinder ion diffusion or cause uneven deposition, thus reducing the efficiency of mechanical strengthening.

Fire Resistance

The fire resistance values of $CaCO_3$ mineralized wood as shown in Fig. 9 were 65.3% for the control, 22.6% for 0.5 mol/L, 16.3% for 1 mol/L, and 19.6% for 2 mol/L. These results demonstrate that mineralization markedly improved fire resistance compared to the untreated control. Specifically, treatments at 0.5 mol/L and 1 mol/L reduced the fire-resistance value to as low as 16% to 23%, indicating significantly enhanced performance. The enhancement can be attributed to the *in-situ* deposition of $CaCO_3$ crystals within the wood matrix, which retard thermal degradation and flame propagation (Hernandez *et al*.

2022). However, at the highest concentration of 2 mol/L, the resistance value slightly increased compared to 1 mol/L, suggesting that overly concentrated mineral deposition may lead to less efficient fire-retardant performance due to pore blockage or uneven mineral distribution (Merk *et al*. 2016; Moya *et al*. 2020). These findings align with previous research showing that controlled mineralization of wood with $CaCO_3$ significantly improves fire retardancy by modifying microstructure and heat-release behaviour (Pondelak *et al*. 2021). Furthermore, studies by Xia *et al*. (2025) and Liu *et al*. (2023) mentioned that interactions between organic and inorganic materials could increase flame retardancy through the formation of carbon layers during combustion. In addition, Geng *et al*. (2025) reported that mineral components can act as a thermal barrier that reduces the combustion rate of materials. This finding is relevant to the $CaCO_3$ mineralization approach used in wood, where the deposited mineral may contribute to improving fire resistance.

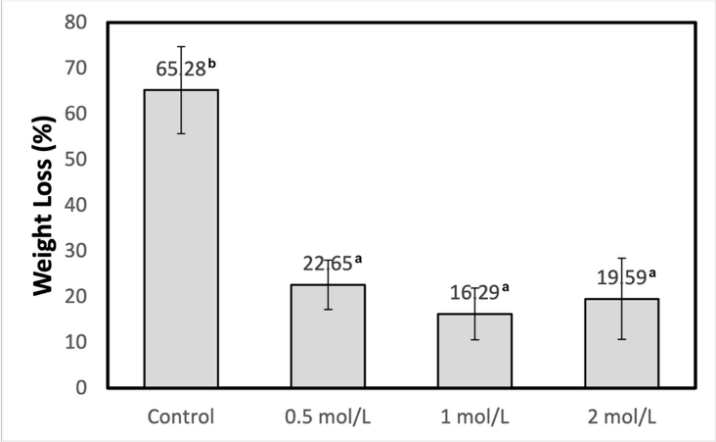

Fig. 9. Fire resistance performance of wood mineralized with $CaCO_3$. Different superscript letters indicate significant differences ($P < 0.05$).

Pores Characterization

The SEM analysis was conducted on eight samples, including untreated (control) and mineralized sengon wood specimens. The control samples exhibited clean cell wall structures with open pores, showing no visible mineral deposition. In contrast, mineralized samples treated with $CaCO_3$ solutions displayed varying degrees of mineral accumulation, indicated by arrows in the SEM images as shown in Fig. 10. At a concentration of 0.5 mol/L, both samples showed clear $CaCO_3$ deposits, with the sapwood sample demonstrating more abundant and evenly distributed deposits due to its larger, more open pores and lower extractive content. As the concentration increased to 1 and 2 mol/L, the amount of visible $CaCO_3$ deposits decreased and became less uniform.

In higher concentrations, the mineral deposits appeared sparser and more irregularly distributed, likely due to oversaturation and potential blocking of pores that hinder further deposition. The SEM observations (Figs. 10g and 10h) revealed that $CaCO_3$ crystals tend to aggregate on the wood surface, while limited deposition is observed within the pores or lumens. This suggests that early crystal agglomeration near the pore openings may partially block the pores and restrict further mineral penetration into the wood structure. Similar limitations in mineral penetration due to particle aggregation have also been reported by Matsunaga *et al*. (2019).

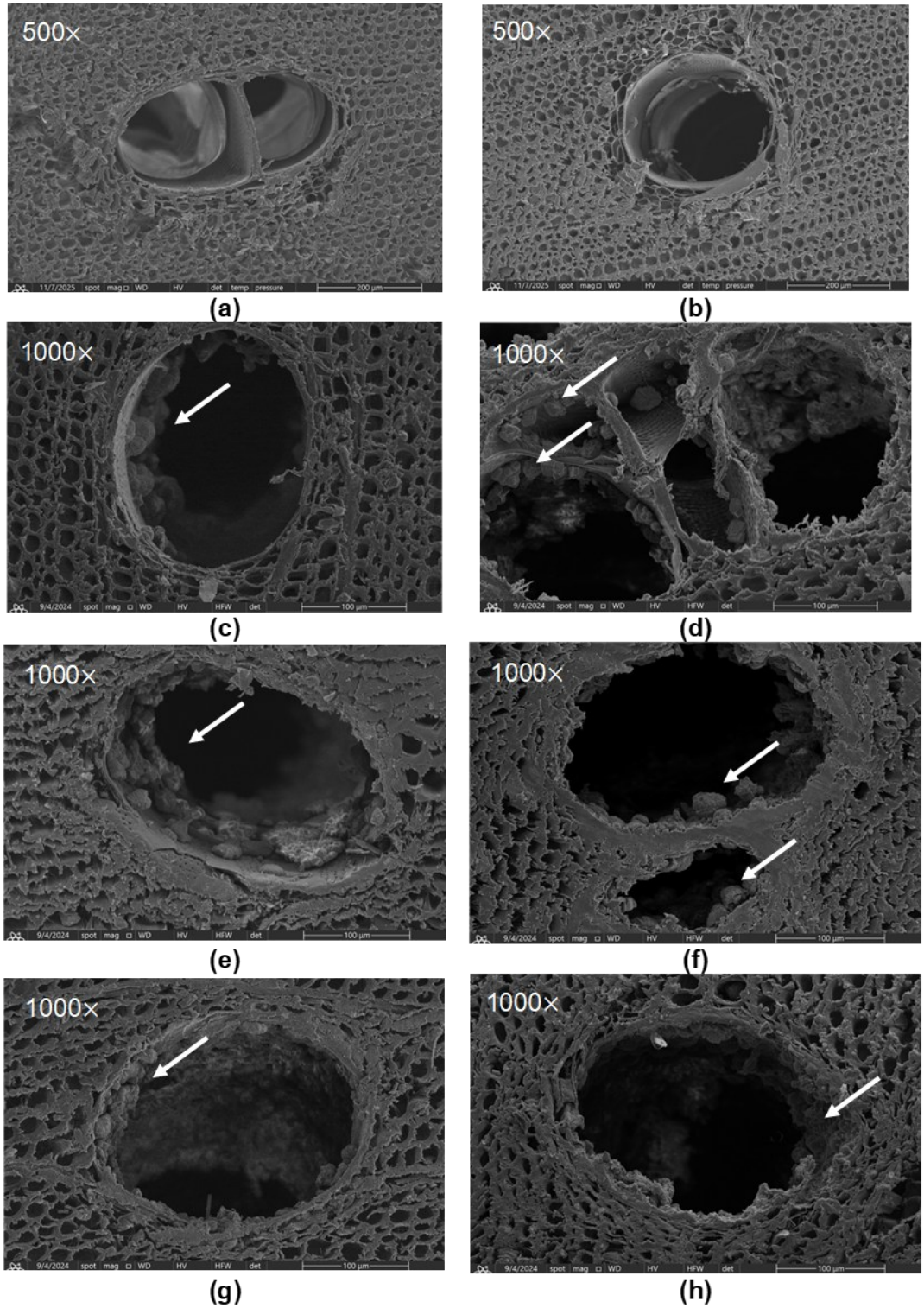

Fig. 10. SEM images showing *in-situ* $CaCO_3$ deposits within the pore structures of the control sample (a, b), and samples impregnated with 0.5 mol/L (c, d), 1 mol/L (e, f), and 2 mol/L (g, h) $CaCl_2/K_2CO_3$ solutions at magnifications of and 500x (a, b) and 1000x (c, d, e, f, g, h). The arrows indicate wood pores filled with $CaCO_3$ deposits.

The crystal structure of control and mineralized sengon wood was examined using X-ray diffraction (XRD). As shown in Fig. 11, the control sample exhibits broad diffraction peaks at around 2θ ≈ 17° and 22°, which correspond to the characteristic peaks of cellulose, indicating that the native wood structure is predominantly amorphous with low crystallinity. After mineralization treatment, the intensity of the cellulose characteristic peaks gradually decreases with increasing concentration, indicating a reduction in cellulose crystallinity after impregnation. In addition to the typical cellulose crystalline planes, additional diffraction peaks begin to appear in all treated samples, particularly in the range of 2θ ≈ 29°, 36°, 39°, 43°, and 47°, which can be attributed to the formation of crystalline $CaCO_3$ (calcite phase). This suggests that the mineralized wood contains various crystalline phases of $CaCO_3$, such as calcite and aragonite, with calcite being the dominant phase due to its highest thermodynamic stability (Zhang *et al*. 2022). Furthermore, noticeable changes in peak shape are observed after mineralization. At concentrations of 0.5 and 1 mol/L, the diffraction peaks become relatively sharper and narrower, although not yet dominant, indicating the initial formation of $CaCO_3$ crystals within the wood matrix in limited amounts and with relatively uniform distribution. In contrast, the most significant change is observed at 2 mol/L, where the diffraction peaks become much sharper, narrower, and more pronounced, particularly around 2θ ≈ 29°, suggesting a higher degree of crystallinity and a more ordered structure due to the increased formation of $CaCO_3$ crystals. However, the highly sharp and intense peaks may also indicate excessive crystal growth and possible agglomeration (Hernandez *et al*. 2025).

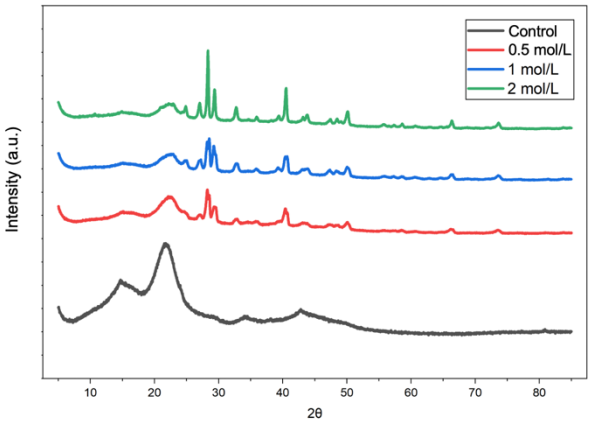

Fig. 11. XRD patterns of control and $CaCO_3$ mineralized sengon wood at different concentrations (0.5, 1, and 2 mol/L), showing the characteristic peaks of cellulose and calcite phases.

CONCLUSION

1. This study investigated the mineralization process using $CaCl_2$ and K_2CO_3 to form $CaCO_3$ and its effects on the physical and mechanical properties of sengon wood. The results demonstrated that $CaCO_3$ mineralization can influence several key properties of the wood.
2. A solution concentration of 0.5 to 1 mol/L provided the most favorable results, showing increased density, higher mineral absorption efficiency, and improvements in flexural strength, stiffness, compressive strength, hardness, and fire resistance. These

improvements are attributed to pore filling and the formation of interactions between mineral deposits and wood cell wall components.

3. In contrast, increasing the concentration to 2 mol/L reduced performance, likely due to mineral agglomeration that limited penetration and affected the internal structure of the wood. Overall, mineralization at moderate concentrations shows potential for improving the performance of fast-growing sengon wood. However, further studies on long-term durability, leaching behavior, and additional fire performance parameters are required before considering broader structural applications

ACKNOWLEDGEMENTS

This research was financially supported by the Directorate General of Research and Development, Ministry of Higher Education, Science, and Technology, under the Research Program Implementation Contract for Fiscal Year 2025 (No. 006/C3/DT.05.00/PL/2025) for the Schemes of Magister Theses Research Funding. The authors also acknowledge the facilities, scientific, and technical support from the Physics and Advanced Imaging Instrument – EM and Spectroscopy Laboratory, National Research and Innovation Agency through E- Layanan Sains, Badan Riset dan Inovasi Nasional.

REFERENCES CITED

ASTM E69-22 (2022). "Standard guide for the use of thermocouples in industrial heating applications," ASTM International, West Conshohocken, PA.

Badan Standardisasi Nasional. (2019). "Metode uji untuk contoh kecil kayu bebas cacat (Test method for small samples of defect-free wood)," *ASTM D143–14, IDT (SNI 8853:2019)*, Badan Standardisasi Nasional, Jakarta, Indonesia.

Chen, C., Chen, J., Zhang, S., Cao, J., and Wang, W. (2020). "Forming textured hydrophobic surface coatings via mixed wax emulsion impregnation and drying of poplar wood," *Wood Science and Technology* 54, 421–439. https://doi.org/10.1007/s00226-020-011567

Choi, H., Dalton, L. E., Peszlen, I., and Pourghaz, M. (2024). "The impacts of $CaCO_3$ deposition in natural wood on its viscoelastic properties," *Composites Part B: Engineering* 281, article 111324. https://doi.org/10.1016/j.compositesb.2024.111324

Delucis, R. A., Cademartori, P. H. G., Missio, A. L., and Gatto, D. A. (2016). "Decay resistance of four fast-growing eucalypts wood exposed to three types of fields," *Maderas. Ciencia y Tecnología* 18(1), 33-42.

Dhami, N. K., Reddy, M. S., and Mukherjee, A. (2013). "Biomineralization of calcium carbonates and their engineered applications: A review," *Frontiers in Microbiology* 4, article 314. https://doi.org/10.3389/fmicb.2013.00314

Divós, F., and Tanaka, T. (2005). "Relation between static and dynamic modulus of elasticity of wood," *Acta Silvatica & Lignaria Hungarica* 1(1), 105-110. https://doi.org/10.37045/aslh-2005-0009

Dunningham, E., and Sargent, R. (2015). *Overview of Emerging International Wood Modification Technologies*, Forest and Wood Products Australia, Melbourne.

Dvořák, O, Sarvašová Kvietková M, Horák P, Kubista K, Pánek M, Štěrbová I. 2023. "Effect of larch wood extractive leaching on accelerated weathering aging durability

of oil-based coatings," *Central European Forestry Journal*. 69(2), 126-131. doi: https://doi.org/10.2478/forj-2022-0018

Fouladi, H. M., Namasivayam, N. S., Hwa, C. C., Xin, P. Z., Xin, S. Y. P., Ghassem, M., and Najafabadi, H. S. (2015). "Enhancement of coir fiber fire retardant property," *Journal of Engineering Science and Technology Special Issue on SOMCHE 2014 and RSCE 2014 Conference* School of Engineering, Taylor's University.

Garskaite, E., Balciunas, G., Drienovsky, M., Sokol, D., Sandberg, D., Bastos, A. C., and Salak, A. N. (2023). "Brushite mineralised Scots pine (*Pinus sylvestris* L.) sapwood – revealing mineral crystallization within a wood matrix by in situ XRD," *RSC Advances* 13, 5813-5825. https://doi.org/10.1039/D3RA00305A

Geng, Q., Yu, Y., Xu, Z., Xie, Y., and Feng, D. (2025). "Enhancing flame retardancy of ethylene-vinyl acetate composites via non-covalent functionalization of black phosphorus nanosheets," *Polymer Degradation and Stability*, 240, article 111433. https://doi.org/10.1016/j.polymdegradstab.2025.111433

Haryanto, A., Hidayat, W., Hasanudin, U., Iryani, D. A., Kim, S., Lee, S., and Yoo, J. (2021). "Valorization of Indonesian wood wastes through pyrolysis: A review," *Energies* 14(5), article 1407. https://doi.org/10.3390/en14051407

Hasnah. (2019). "Effects of *in situ* polymerization on water repellency and dimensional stability of modified wood: Assessment using ASE," *Holzforschung* 73(5), 417-428. https://doi.org/10.1515/hf-2019-0176

He, Y., Xie, G., Li, X., and Li, Q. (2024). "Fabrication of highly stable and durable wood materials by modification of polyacrylamide (PAM)–glyoxal (GLY)," *Industrial Crops and Products* 222, article 120033. https://doi.org/10.1016/j.indcrop.2024.120033

Hernandez, V., Romero, R., Arias, S., and Contreras, D. (2022). "A novel method for calcium carbonate deposition in wood that increases carbon dioxide concentration and fire resistance," *Coatings* 12(1), 72. https://doi.org/10.3390/coatings12010072

Hernandez, V. A., Ovalle, C., Fuentes, S., and Núñez-Decap, M. (2025). "$CaCO_3$ radiata pine wood mineralization: Weathering and mold resistance, and effect on mechanical and adhesion properties," *Forests* 16(2), article 233. https://doi.org/10.3390/f16020233

Hill, C. (2006). *Wood Modification: Chemical, Thermal and Other Processes*, Wiley Series on Renewable Resources, Chapter 5, 99-127.

Holy, S., Temiz, A., Köse Demirel, G., Aslan, M., and Mohamad Amini, M. H. (2022). "Physical properties, thermal and fungal resistance of Scots pine wood treated with nano-clay and several metal-oxides nanoparticles," *Wood Material Science and Engineering* 17(3), 176-185. https://doi.org/10.1080/17480272.2020.1836023

Iswanto, A. H. (2018). "Physical properties of wood: Specific gravity and moisture content in several wood species," *Jurnal Kehutanan* 4(2), 4-5.

Jiang, J., Wang, C., Ebrahimi, M., Shen, X., and Mei, C. (2022). "Eco-friendly preparation of high-quality mineralized wood via thermal modification induced silica sol penetration," *Industrial Crops and Products* 183, article 115003. https://doi.org/10.1016/j.indcrop.2022.115003

Jirouš Rajković, V., and Miklečić, J. (2021). "Enhancing weathering resistance of wood—A review," *Polymers* 13(12), article 1980. https://doi.org/10.3390/polym13121980

Karlinasari, L., Wahyuna, M. E., and Nugroho, N. (2008). "Non-destructive ultrasonic testing method for determining bending strength properties of Gmelina wood (*Gmelina arborea*)," *Journal of Tropical Forest Science* 2008, 99-104.

Karlinasari, L., Lestari, A. T., and Priadi, T. (2018). "Evaluation of surface roughness and wettability of heat-treated, fast-growing tropical wood species sengon (*Paraserianthes falcataria* (L.) Nielsen), jabon (*Anthocephalus cadamba* (Roxb.) Miq.), and acacia (*Acacia mangium* Willd.)," *International Wood Products Journal*, 2018, 1-7.

Kraigher, H., Humar, M., and Gričar, J. (2023). *Gozd in les: Gozd prihodnosti* (*Forest and Wood: The Forest of the Future*), In: *Proceedings of the Zbornik Recenziranih Znanstvenih Prispevkov Na Domači Konferenci Gozd in Les: Gozd Prihodnosti*, Gozdarski Inštitut Slovenije, Ljubljana, Slovenia, p. 54.

Kumari, D., Qian, X.-Y., Pan, X., Achal, V., Li, Q., and Gadd, G. M. (2016). "Microbially-induced carbonate precipitation for immobilization of toxic metals," *Advances in Applied Microbiology* 94, 79-108. https://doi.org/10.1016/bs.aambs.2015.12.002

Laksono, G. D., Rahayu, I. S., Karlinasari, L., Darmawan, W., and Prihatini, E. (2023). "Characteristics of magnetic sengon wood impregnated with nano Fe_3O_4 and furfuryl alcohol," *Wood Science and Technology.* https://orcid.org/0000-0003-4902-564X

Liu, X., Fang, X., Sun, C., Zhang, T., Wang, K., and Dong, Y. (2023). "Hybrid wood composites with improved mechanical strength and fire retardance due to a delignification–mineralization–densification strategy," *Forests* 14(8), article 1567. https://doi.org/10.3390/f14081567

Liang, D., Ding, Z., Yan, Q., Hasanagić, R., Fathi, L., Yang, Z., Li, L., Wang, J., Luo, H., Wang, Q., and Chu, D. (2022). "A primary study on mechanical properties of heat-treated wood via *in-situ* synthesis of calcium carbonate," *Journal of Renewable Materials* 10(11), 2915-2929. https://doi.org/10.32604/jrm.2022.023214

Madhoushi, M., and Boskabadi, Z. (2019). "Relationship between the dynamic and static modulus of elasticity in standing trees and sawn lumbers of *Paulownia fortune* planted in Iran," *Maderas. Ciencia y Tecnología* 21(1), 35-44. https://doi.org/10.4067/S0718-221X2019005000104

Matsunaga, H., Kiguchi, M., and Evans, P. D. (2009). "Microdistribution of copper carbonate and iron oxide nanoparticles in treated wood," *Journal of Nanoparticle Research* 11, 1087-1098. https://doi.org/10.1007/s11051-008-9512-y

Merk, V., Chanana, M., Keplinger, T., Gaan, S., and Burgert, I. (2015). "Hybrid wood materials with improved fire retardance by bio-inspired mineralisation on the nano- and submicron level," *Green Chemistry* 17, 1423-1428. https://doi.org/10.1039/C4GC02158D

Merk, V., Chanana, M., Gaan, S., and Burgert, I. (2016). "Mineralization of wood by calcium carbonate insertion for improved flame retardancy," *Holzforschung* 70(9), 867-876. https://doi.org/10.1515/hf-2015-0217

Moya, R., Gaitán-Alvarez, J., Berrocal, A., and Araya, F. (2020). "Effect of $CaCO_3$ on the wood properties of tropical hardwood species from fast-growth plantation in Costa Rica," *BioResources* 15(3), 4802-4822. https://doi.org/10.15376/biores.15.3.4802-4822

Mustoe, G. E. (2017). "Wood petrifaction: A new view of permineralization and replacement," *Geosciences* 7(4), article 119. https://doi.org/10.3390/geosciences7040119

Mustoe, G. E. (2023). "Silicification of wood: An overview," *Minerals* 13(2), article 206. https://doi.org/10.3390/min13020206

Pondelak, A., Škapin, A. S., Knez, N., Knez, F., and Pazlar, T. (2021). "Improving the flame retardancy of wood using an eco-friendly mineralisation process," *Green Chemistry*, 23(3):1130-1135. https://doi.org/10.1039/D0GC03852K

Rahayu, I., Darmawan, W., Zaini, L. H., and Prihatini, E. (2019). "Characteristics of fast-growing wood impregnated with nanoparticles," *Journal of Forestry Research*, 31(2), 677-685. https://doi.org/10.1007/s11676-019-00902-3

Rahayu, I., Riadhi, M. R., Wahyuningtyas, I., Prihatini, E., and Ismail, R. (2024). "Mechanical properties and durability of impregnated sengon wood using monoethylene glycol and SiO_2 nanoparticles," *Journal of Sylva Indonesiana* 7(2), 110-121. https://doi.org/10.32734/jsi.v7i02.15729

Repič, R., Pondelak, A., Kržišnik, D., Humar, M., and Sever Škapin, A. (2022). "Combining mineralisation and thermal modification to improve the fungal durability of selected wood species," *Journal of Cleaner Production* 2022, article 131530. https://doi.org/10.1016/j.jclepro.2022.131530

Rodriguez-Navarro, C., Jroundi, F., Schiro, M., Ruiz-Agudo, E., and González-Muñoz, M. T. (2012). "Influence of substrate mineralogy on bacterial mineralization of calcium carbonate: Implications for stone conservation," *Applied and Environmental Microbiology* 78(11), 4017-4029. https://doi.org/10.1128/AEM.07044-11

Shalbafan, A., and Thoemen, H. (2023). "Development of mineral-bonded plywood with magnesium oxychloride as a binder using the hot-pressing process," *Polymers* 15(4), 805. https://doi.org/10.3390/polym15040805

Soini, S. A., Lalani, I., Maron, M., Gonzalez, D., Mahfuz, H., Domingo, N., and Merk, V. (2025). "Multiscale mechanical characterization of mineral-reinforced wood cell walls," *ACS Applied Materials and Interfaces* 17(12), 18887-18896. https://doi.org/10.1021/acsami.4c22384

Tao, Y., Li, P., Cai, L., and Shi, S. Q. (2019). "Flammability and mechanical properties of composites fabricated with $CaCO_3$-filled pine flakes and phenol formaldehyde resin," *Composites Part B: Engineering* 167, 1-6. https://doi.org/10.1016/j.compositesb.2018.12.005.

Xia, Y., Zhang, X., An, L., Xie, Y., Wu, F., Mei, Y., Xie, D., and Feng, D. (2025). "Synergistic flame retardancy of cross-linked kraft lignin and black phosphorus on TPU: Mechanism and performance," *Chemical Engineering Journal* 519, article 165178. https://doi.org/10.1016/j.cej.2025.165178

Xu, E., Wang, D., and Lin, L. (2020). "Chemical structure and mechanical properties of wood cell walls treated with acid and alkali solution," *Forests* 11(1), article 87. https://doi.org/10.3390/f11010087

Zhang, M., Li, H., Wang, C., Wang, Z., Liu, D., Yang, T., Deng, Z., and Yuan G. (2022). "Performance enhancement of the poplar wood composites biomimetic mineralized by $CaCO_3$,"*ACS Omega* 7, 29465-29474.

Article submitted: November 18, 2025; Peer review completed: March 7, 2026; Revised version received: March 18, 2026; Accepted: April 24, 2026; Published: April 30, 2026.
DOI: 10.15376/biores.21.2.5351-5369